

Damage Visualization of Imperfectly-Grouted Sheath in PC Structures

Satoshi OSAWA *, Tomoki SHIOTANI **, Hisato KITORA ***,
Yoshiyuki MOMIYAMA ***

* Dept. of Urban Management, Kyoto University
E-mail: oosawa.satoshi.88w@st.kyoto-u.ac.jp

** Dept. of Civil and Earth Resources Engineering, Kyoto University
E-mail: shiotani.tomoki.2v@kyoto-u.ac.jp

*** West Nippon Expressway Engineering Kansai Co., Ltd
E-mail: h_kitora@w-e-kansai.co.jp
E-mail: momiyama@w-e-kansai.co.jp

Abstract. In recent years, PC cables' breakage due to corrosion is reported frequently in post-tensioned PC structures. It can be considered that the imperfectly-grouted sheath is the principal cause, leading to eventual failure in the worst case. The techniques to diagnose the imperfectly-grouted sheath in post-tensioned PC structures is thus in high demand. Conventionally NDT such as ultrasonic technique, SIBIE and AE monitoring have been applied for the diagnosing the deterioration of PC structures [1], but there are still many issues to solve with respect to the accuracy and quantitative evaluation for the degradation, so that the visual check, which is the most reasonable and convenient but can be applied only for the surface deterioration is well used to diagnose, regarding as the representative of the general deterioration in the present circumstances. To solve these issues, the authors have tried to identify the imperfectly-grouted sheath in post-tensioned PC specimens by elastic wave tomography [2], which has been studied enthusiastically in author's group exhibiting the high-accurate results of damage identification [3]. In order to determine the both of the adequate arrangement of AE sensors and the effective frequency of the elastic wave transmission [4], numerical simulations were implemented in advance of the experimental approaches. In this paper, the both result of simulation and experiment for imperfectly-grouted sheath, subjected to elastic wave tomography are showed and finally some compatible results could be obtained. As a result, it was possible to identify imperfectly-grouted sheath in the post-tensioned PC specimen by elastic wave tomography. Several issues to improve the accuracy of the elastic wave tomography were cleared successfully in application of the elastic wave tomography for the diagnosis of the grouting condition between the sheath and tendons on in-situ PC structure.

1. Introduction

The dense injection of cementitious grout into the sheath is necessary in post-tensioned PC structures for connecting the steel tendon with the concrete material of PC structures as well as preventing the steel tendon from being corroded. However in the aging PC structures, infiltration of rain to the voids in the sheath induced by improper grouting can lead to the corrosion of PC tendons, the deterioration of load resistance capability and remarkable



damage around the structures in the worst case. In recent years, a lot of accidents associated with the deterioration of PC structures were confirmed, caused by improper grouting in many cases. In order to solve this issue, the establishment of proper NDT to evaluate the grouting condition is thus in high demand.

As a method for examining the imperfectly-grouted sheath from the surface of PC structures, a lot of methods such as X-ray methods, SIBIE, impact elastic-wave methods and electromagnetic pulse methods have been studied so far [5]; however, they have many issues to solve in applications to in-situ structures with respect to the area of measurement, promptness of testing and accuracy of the test results.

In this study, as a method for examining the imperfectly-grouting area in PC structures effectively in advance of becoming the fatal deterioration, the applicability of the elastic wave tomography, which has been applied for breakage-evaluation PC tendons in the past study [6] and could accurately examine them in the wide area, was tried to apply. Firstly the numerical simulation was implemented, followed by some experiments to examine the reasonable experimental condition as for the excitation frequency and the array of sensors. Based on the obtained experimental proper condition from the numerical simulation, the experiment was conducted. Comparing the results in both of the numerical simulation and experiment, the applicability of elastic wave tomography for examining imperfectly-grouted sheath in PC structures was verified. In practice, four types of ultrasonic waves having the different frequency respectively were excited in order to verify the effect by the differences of the frequency of elastic wave transmission.

2. Elastic Wave Tomography

Elastic wave tomography is a method for evaluating the characteristic of elastic waves in each element over the structure through variations of elastic waves parameters from a source to multiple receivers located at different positions of the target structure. Several elastic wave parameters in each element such as elastic wave velocity and the attenuation ratio of amplitude are obtained through the tomography. Among those, the elastic wave velocity has been well used to relate the deterioration because the elastic waves are regarded to be associated with the elastic moduli, implying the information of internal damages such as voids in the materials. In this study, this elastic wave velocity was thus used for the elastic wave tomography. When there are voids, the elastic waves will exhibit manners of scattering, reflection and diffraction, as a result; the elastic wave velocity will decrease. This theory supports in the algorithm of elastic wave tomography. A brief description of the algorithm can be found below.

Firstly the propagation velocity of the elastic wave is calculated by both of the distance from the excitation point to the receive point and T_{OBS} (observed propagation time) obtained by Eq. 1:

$$T_{OBS} = t_o - t_s \quad (1)$$

where t_s is the excitation time and t_o is the arrival time.

On the other hand, in the algorithm of the elastic wave tomography, the inverse of velocity, or specifically referred to as the “slowness” is given as an initial parameter into each element as shown in Fig. 1. Then T_{CAL} (theoretical propagation time) obtained by a finite element model is the total of the propagation time calculated by the slowness and the distance in each element (see Eq. 2). And ΔT which defines the difference between observed propagation time and theoretical propagation time is obtained by Eq. 3:

$$T_{CAL} = \sum_j s_j l_j \quad (2)$$

$$\Delta T = T_{OBS} - T_{CAL} \quad (3)$$

where l_j is the length crossing each element and s is the slowness.

Then the slowness in each element is revised in order to reduce the difference between observed propagation time and theoretical propagation time. The slowness correction amount is obtained by means of the SIRT method (Simultaneous Iterative Reconstruction Technique). The slowness correction amount in each element and the revised slowness are obtained by Eq. 4 and 5:

$$\begin{Bmatrix} \Delta s_1 \\ \Delta s_2 \\ \vdots \\ \Delta s_j \end{Bmatrix} = \begin{bmatrix} \sum_i \frac{\Delta T_i l_{i1}}{L_i} / \sum_i l_{i1} \\ \sum_i \frac{\Delta T_i l_{i2}}{L_i} / \sum_i l_{i2} \\ \vdots \\ \sum_i \frac{\Delta T_i l_{ij}}{L_i} / \sum_i l_{ij} \end{bmatrix} \quad (4)$$

$$s'_j = s_j + \Delta s_j \quad (5)$$

where L_i is the total distance of the wave in the i -element.

This algorithm enables to calculate the slowness, or the velocity in each element corresponding to the observed propagation time of multiple waves over the structure, resulting in forming the contour map of the elastic wave velocity over the target area.

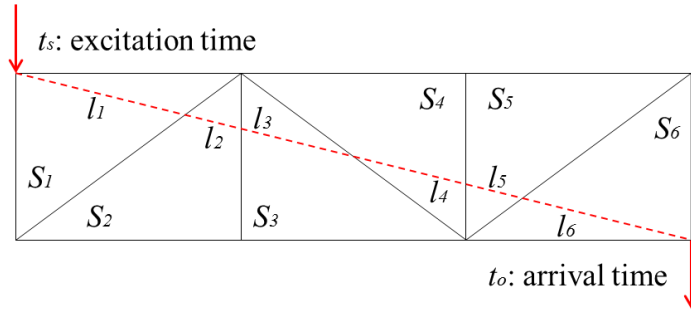


Fig. 1. The configuration of calculation of propagation time

3. Numerical Simulation

Numerical simulations, which were fundamentally conducted in order to evaluate the grouting condition in the sheath with the elastic wave tomography, are implemented in this chapter.

3.1 Analysis Condition

In this numerical simulation, “Wave 2000” (Cyber Logic) was used as a numerical simulation software. This software calculates an approximate value with regard to two-dimensional elastic wave equation, specifically uses FDM (finite difference method) and elastic wave equation as shown in Eq. 6:

$$\rho \frac{\partial^2 w}{\partial t^2} = \left[u + \eta \frac{\partial}{\partial t} \right] \nabla^2 w + \left[\lambda + \mu + \phi \frac{\partial}{\partial t} + \frac{\eta}{3} \frac{\partial}{\partial t} \right] \nabla (\nabla \cdot w) \quad (6)$$

where ρ is the material density, λ and μ are the first and second Lamé constants respectively, η is coefficient of shear viscosity, ∇ is the gradient operator, $\nabla \cdot$ is the divergence operator and t is the travel time.

In this numerical simulation, a cross section of the target structure was set as shown in Fig. 2. The cross section has 250 mm in height and 300 mm in width, which is identical with the cross section of the specimen in the experiment. Both of the steel sheath and the plastic sheath was set as the sheath material in the structure. The sheath has 38 mm in external diameter and 1 mm in thickness, and the PC tendon has 32 mm in diameter. They are located 95 mm lower from the upper end of the structure and in the middle in transverse direction. For verifying the effect to the elastic waves by the difference of the grouting ratio, three kinds of grouting ratio (0%, 50% and 100%) was set as shown in Fig. 3. Table 1 shows the physical property of each material.

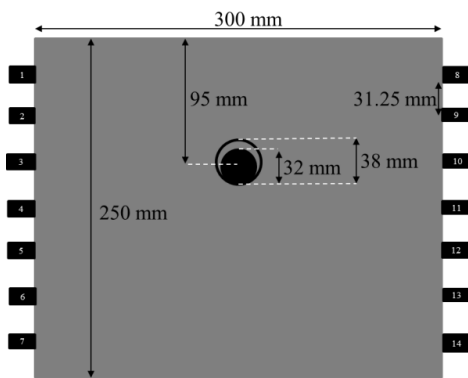


Fig. 2. The cross section of the target structure

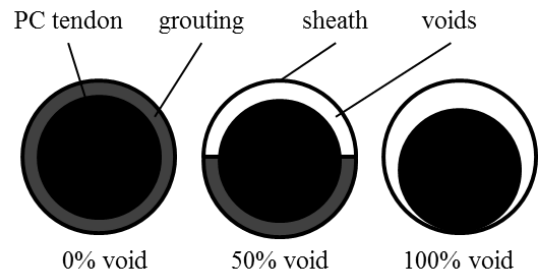


Fig. 3. The grouting ratio

Table 1. The physical property of each material

Physical property	Concrete	Grout	Air Dry @20 Degree	Iron	Polyethylene
ρ (kg/m ³)	2380	2236	1.24	7690	900
λ (MPa)	9874.61	7500	0.14674	110149	6500
μ (MPa)	13636.4	11250	0	78750	260
vL (m/s)	3950.72	3662.9	344.004	5900.12	2792.85

3.2 Sensor Arrangement and Cell Division

The length of waves passing through each cell is one of the most important factors in relation to verifying the accuracy of the elastic wave tomography. Then our group defined a value namely the total wave length in a cell divided by the area of the cell, as the “wave density” and it has been used as a parameter with regard to the verification of the accuracy of elastic wave tomography.

Figure 2 also shows the arrangement of AE sensors for elastic wave tomography. In this numerical simulation, seven AE sensors were installed onto the each side respectively and the space between each two sensors was set to 31.25 mm in order to examine the grouting condition in the sheath in detail. As shown in Fig. 4, the cross section area was divided into 160 cells. Especially the central area including the sheath and the PC tendon was divided into smaller parts in order to calculate the elastic wave velocity in detail as shown in Fig. 5. For verifying the accuracy of elastic wave tomography, the wave density of each cell was

calculated (see Fig. 6). In the past study, when wave density is larger than 0.5 cm/cm^2 , the accurate verification can be possible. According to Fig. 6, it is obvious that the adapted cell division has sufficient accuracy for elastic wave tomography. Correspondingly the sensor arrangement and the cell division set above were used for this study.

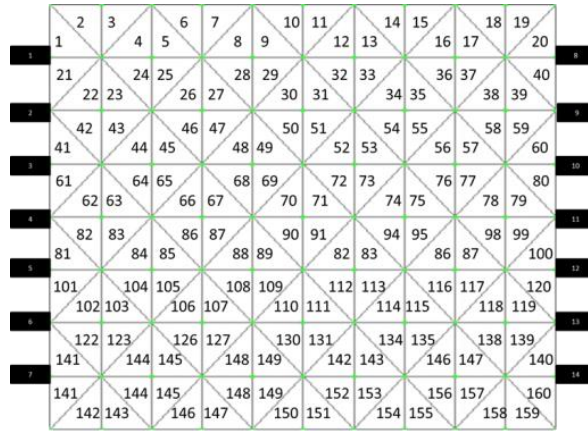


Fig. 4. The cell division in the whole area

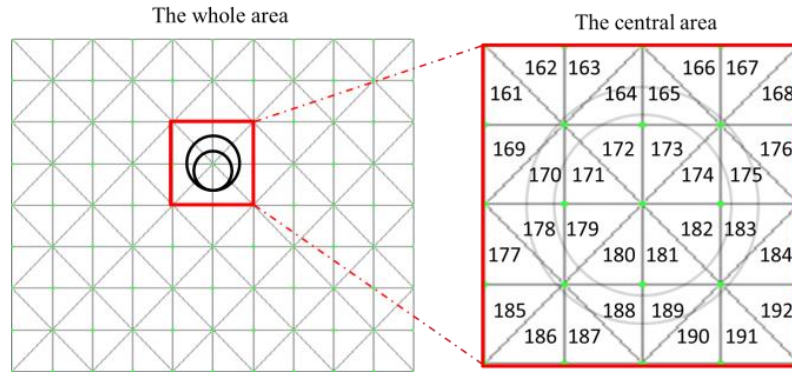


Fig. 5. The cell division in the central area

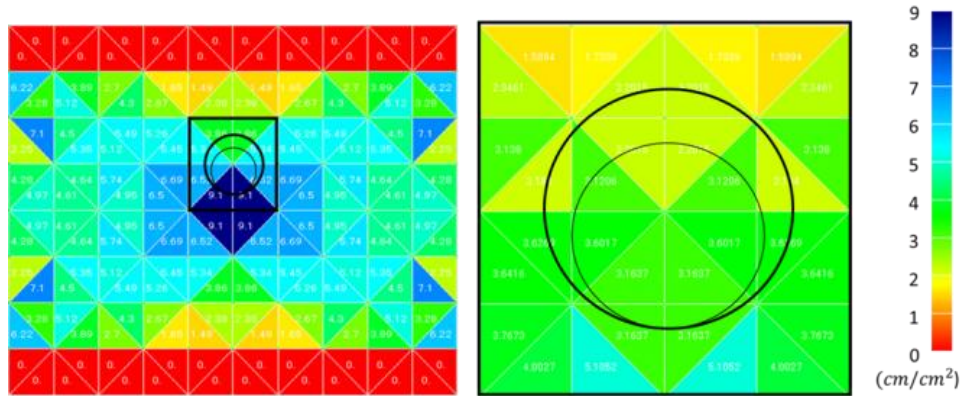


Fig. 6. The wave density in each cell

3.3 The Result of Numerical Simulation

The velocity contour was drawn based on the elastic wave tomography using the arrival time differences among AE sensors. In this study, two kinds of elastic waves comprised of 20 kHz and 1 MHz were respectively transmitted as the excitation frequency in order to evaluate the effect to waves by the differences of frequency. Figure 7 -10 show the result of elastic wave tomography. In the cases of the steel sheath (see Figs. 7 and 8), the decrease of elastic wave velocity was confirmed as increase of grouting void ratio; however, there was not much

difference between in the case of 1 MHz and 20 kHz. While in the case of the plastic sheath (see Figs. 9 and 10), the smaller elastic wave velocity was, the larger the grouting void ratio becomes, suggesting better relation between the velocity and the void ratio than that in the case of the steel sheath; however, remarkable difference in excitation frequency couldn't be confirmed as same as in the steel sheath. As a result of these contours, it is obvious that the deterioration of elastic wave velocity corresponds well to the decrease of grouting ratio; however, the differences by frequency couldn't be verified. Especially, it is noted that there are apparent differences between grouting ratio 0% and 50%, 100%, correspondingly completely empty namely 100% void condition of the grout can be possible to evaluate with the elastic wave tomography.

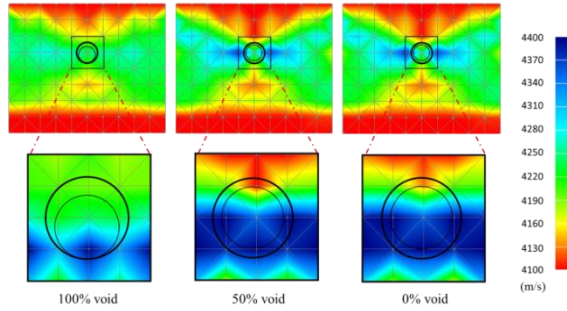


Fig. 7. The result of elastic wave tomography in the case of steel sheath with 1 MHz frequency

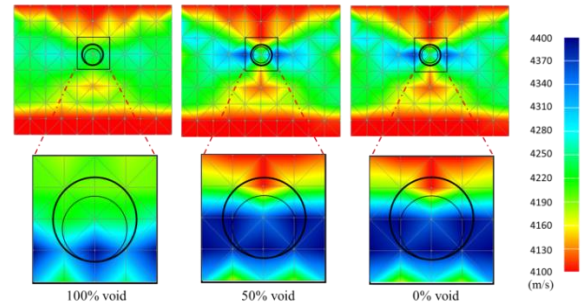


Fig. 8. The result of elastic wave tomography in the case of steel sheath with 20 kHz frequency

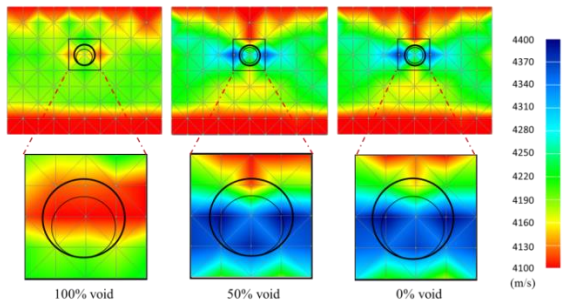


Fig. 9. The result of elastic wave tomography in the case of plastic sheath with 1 MHz frequency

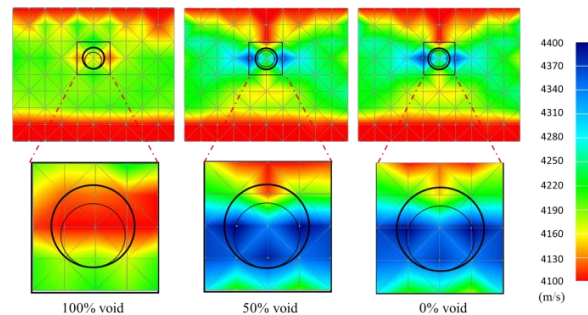


Fig. 10. The result of elastic wave tomography in the case of plastic sheath with 20 kHz frequency

4. Experiment

4.1 Experimental Overview

The concrete specimen has 250 mm in height, 300 mm in width and 500 mm in length. Seven AE sensors (resonant frequency of 150 kHz) were installed onto the each side respectively as shown in Fig. 11. The arrangement of AE sensors was same as one of the numerical simulation. The sinusoidal waves generated by the function-generator (Tektronix) were amplified 20 times as much as the original one with the amplifier (Piezo Systems). The AEWIn (PAC) was used for processing AE (acoustic emission) waveforms. Figure 12 shows these measurement instruments. In this experiment, two kinds of sheath materials (steel or plastic) and 7 specimens comprised of three types of grouting ratio (0%, 50% and 100%) and no sheath were prepared. Four types of excitation frequency (20 kHz, 50 kHz, 200 kHz and 1 MHz) were generated respectively.



Fig. 11. The arrangement of AE sensors

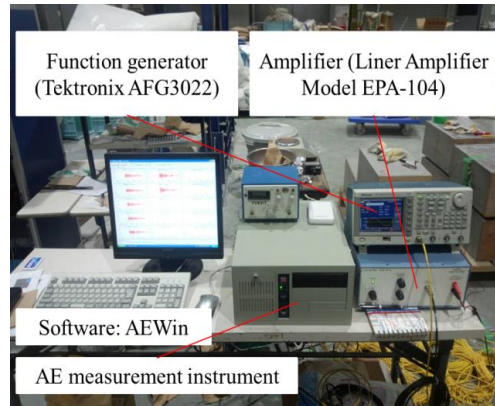


Fig. 12. AE measurement instruments

4.2 The Result of Experiment

As one example, the result of elastic wave tomography in the case of steel sheath and 200 kHz excitation frequency are shown as in Fig. 13. Rough evaluation for the void condition could be implemented, then to quantify the void condition, the average of elastic wave velocity in the vicinity of the sheath, namely the area surrounded by the red lines as shown in Fig. 14 is calculated. Integrating the results obtained by all the specimens and excitation frequency, they are shown as in Figs. 15 and 16.

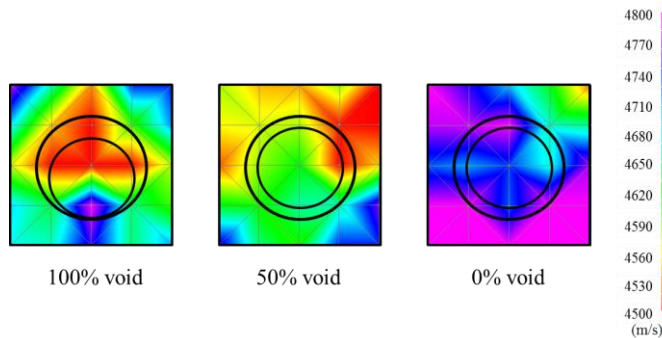


Fig. 13. The result of elastic wave tomography in the steel sheath with 200 kHz frequency

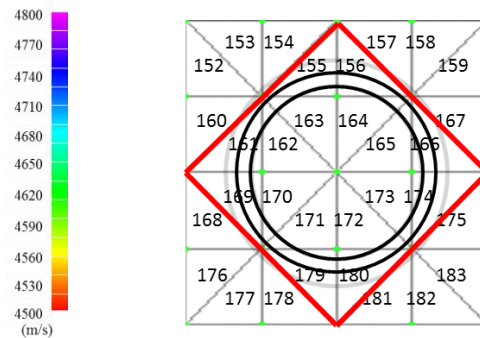


Fig. 14. Averaging elastic wave velocity surrounded by red lines

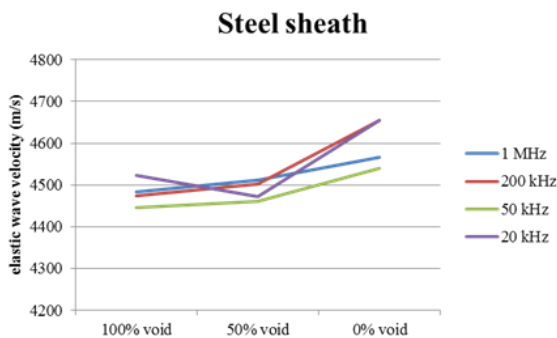


Fig. 15. The average elastic wave velocity in the case of the steel sheath

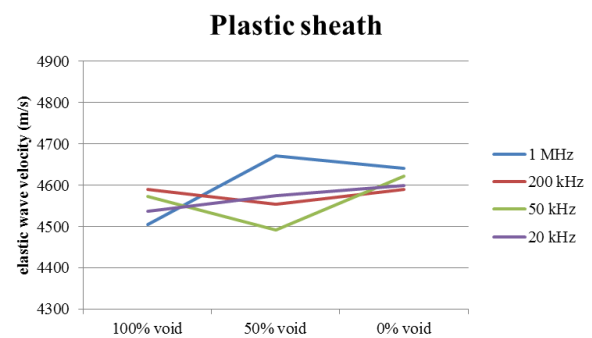


Fig. 16. The average elastic wave velocity in the case of the plastic sheath

In the case of the steel sheath, the increase of elastic wave velocity corresponding to the decrease of void ratio could be confirmed in almost all excitation frequency. While in the case of the plastic sheath, elastic wave velocity didn't have good relation to the grouting ratio; however, comparing the results in 0% and 100% void, there confirmed the definite

difference. As the thickness of the plastic sheath used in the experiment (2 mm) was larger than one of the steel sheath (0.5 mm), there were differences of the acoustic impedance between the plastic and steel sheath material, which might be attributed to the elastic wave velocity variation, the internal diagnosis. Correspondingly it is concluded that it can be possible to quantify the grouting condition in the case of the steel sheath, while only two sides diagnosis if it was fully filled or not can be determined in the case of the plastic sheath with the elastic wave tomography.

5. Conclusions

In this study, the elastic wave tomography was used for evaluating the grouting condition in the sheath of PC structures. The applicability of elastic wave tomography was tried to verify by means of the numerical simulation and the experiment. Based on this study, conclusions can be made as follows:

- In the case of the steel sheath, the decrease of elastic wave velocity could be confirmed in accordance with the decrease of grouting ratio.
- In the case of the plastic sheath, it can be possible to distinguish grouting ratio 0% from grouting ratio 100%. In the numerical simulation, the results in the case of the plastic sheath show the better relation to the decrease of elastic wave velocity than the ones in the case of the steel sheath. In order to solve this issue, it is necessary to examine the thickness of the sheath and the differences of acoustic impedance of two sheath materials.

In this study, it was confirmed that it could be possible to verify the deterioration of grouting ratio with the elastic wave tomography. However the obtained elastic wave velocity shows slight differences between maximum values and minimum values, the applicability isn't always accurate in the actual structures in which a lot of measurement errors are anticipated. In the future, considering the change of central frequency and the damping ratio of energy parameter such as amplitude, which can evaluate the internal damages sensitively, the evaluation of grouting condition should be conducted. Subsequently, the verification in in-situ structures is scheduled to be implemented.

References

- [1] Alver, N., Tokai, M., Nakai, Y. and Ohtsu, M.: Identification of imperfectly-grouted tendon-duct in concrete by SIBIE procedure, International Conference on NDE for Safety, pp. 9-14, Prague, Czech Republic, November, 2007.
- [2] Momoki, S., Chai, H. K., Shiotani, T., Kobayashi, Y. and Miyanaga, T.: Evaluation of concrete structures with three-dimensional elastic wave tomography, *Journal of Structural Engineering*, Vol. 57A, pp. 959-966, 2011. (in Japanese)
- [3] Momoki, S., Shiotani, T., Chai, H. K., Aggelis, D. G. and Kobayashi, Y.: Large-scale of concrete repair by three-dimensional elastic-wave based visualization technique, *SAGE, Structural Health Monitoring*, Vol. 12, pp. 240-251, 2013.
- [4] Aggelis, D. G., Tsimpris, N., Chai, H. K., Shiotani, T. and Kobayashi, Y.: Numerical simulation of elastic waves for visualization of defects, *Construction and Building Materials*, Vol. 25, pp. 1503-1512, 2011.
- [5] Kamada, T., Uchida, S., Tsunoda, H. and Sato K.: Non-destructive evaluation methods for grouting condition in tendon ducts in existing prestressed concrete bridges, *Journal of JSCE, Division E: Materials, Concrete Structures and Pavement*, Vol. 68, No. 4, pp. 238-250, 2012. (in Japanese)
- [6] Liu, K. F., Chai, H. K., Nima, M., Kobayashi, Y. and Shiotani, T.: Condition assessment of PC tendon duct filling by elastic wave velocity mapping, *The Scientific World Journal*, Vol. 2014, Article ID 194295, 14 pages, 2014.